SYNTHESIS AND PHYSICOCHEMICAL STUDY OF THE $Ag_{8-x}SnSe_{6-x}I_x$ SOLID SOLUTIONS

N.A. Bayramova*[1], I.F. Huseynova[2], K.N.Babanly[2], N.M.Allazova[2], N.B.Babanly[3], M.Bulanova[4], S.Z.Imamaliyeva[2]

[1]Nakhchivan State University, Nakhchivan, Azerbaijan
[2] "Institute of Chemistry" Public Legal Entity, MSE of the Azerbaijan Republic, Baku, Azerbaijan
[3]Baku State University, Gazakh Branch
[4]I.M.Frantsevich Institute for Problems of Materials Sciences, National Academy of Sciences of Ukraine, Kyiv, Ukraine

nurtenbayramova123@gmail.com

Received 22.02.2026
Reviewed 01.04.2026
Accepted 30.04.2026

The results of the investigation of phase equilibria in the Ag_8SnSe_6-Ag_7SnSe_5I system by differential thermal analysis and X-ray phase analysis are presented. It was established that the Ag_8SnSe_6-Ag_7SnSe_5I system is characterized by the formation of a continuous series of solid solutions between Ag_7SnSe_5I and the high-temperature cubic modification of Ag_8SnSe_6, as well as limited solid solutions based on the low-temperature modification of the latter compound. The formation of solid solutions leads to a decrease in the polymorphic transition temperature of Ag_8SnSe_6 and stabilization of the high-temperature cubic phase at room temperature. The obtained results are of interest from the viewpoint of crystal growth of solid solutions with Se↔I substitution in the Ag_8SnSe_6-Ag_7SnSe_5I system.

Keywords: argyrodite family compounds, silver–tin selenoiodide, phase equilibria, solid solutions, T–x diagram.

https://doi.org/10.59849/0005-2531.2026.3.37

1. Introduction

Argyrodite-type compounds with the general formula $A^{m+}_{(12-n)/m}B^{n+}X^{2-}_{6-x}Y^{-}_{x}$ (A^{m+} -Cu^+, Ag^+, Li^+, Zn^{2+}, Cd^{2+}, Hg^{2+}; B^{n+} - Ga^{3+}, Si^{4+}, Ge^{4+}, Sn^{4+}, P^{5+}, As^{5+}; X^{2-} - S^{2-}, Se^{2-}, Te^{2-}; Y^- - Cl^-, Br^-, I^-) [1–3] are characterized by a broad spectrum of functional properties owing to their structural and compositional flexibility.

Compounds of this class exhibit anomalously low lattice thermal conductivity with weak temperature dependence, while the rigid anionic framework ensures charge transport characteristic of conventional semiconductors. As superionic conductors comprising two structurally independent subsystems — a rigid anionic framework and weakly bonded Cu^+ (Ag^+) cations — these materials are considered a promising platform for the design of highly efficient thermoelectric systems through independent tuning of electrical and thermal transport properties [4–9]. Cubic argyrodite phases, distinguished by high ionic conductivity, are of considerable interest for applications as ion-selective electrodes, sensors, solid electrolytes, and other functional devices [10–13]. Furthermore, these compounds exhibit notable optical [9, 14, 15] and photovoltaic properties [16–18].

The search for novel multicomponent phases of variable composition is generally

carried out by increasing the chemical complexity of already known functional compounds. In this context, systematic investigations of phase equilibria in relevant systems are of particular importance. As is well known, phase diagrams not only describe the coexistence of phases within a system, but also provide insight into phase formation mechanisms, thermal stability, primary crystallization and homogeneity regions, as well as polymorphic transformations and other specific features of the system [19–22].

Complex systems based on ternary copper- and silver-containing argyrodites have been investigated in a number of studies, and their phase diagrams have been constructed [4, 22–32]. However, analogous systems containing halogen-substituted argyrodites, despite their attractive functional properties [9–11, 14], remain insufficiently explored [33–36].

The present work is devoted to the investigation of phase equilibria in the Ag_8SnSe_6–Ag_7SnSe_5I system, as well as to the synthesis and characterization of solid solutions with compositions $Ag_{8-x}SnSe_{6-x}I_x$ (x = 0.2–0.8).

The Ag_8SnSe_6 compound melts congruently at 1015 K and undergoes a polymorphic transformation at 355 K [25, 37, 38]. The high-temperature modification (HT) crystallizes in the cubic system (space group $F\bar{4}3m$, a = 1.112 nm), whereas the low-temperature modification (RT) crystallizes in the orthorhombic system (space group $Pmn2_1$, a = 0.79168(6), b = 0.78219(6), c = 1.10453(8) nm) [2, 39].

To the best of our knowledge, no literature data are available concerning the melting temperature and crystallographic parameters of the Ag_7SnSe_5I compound.

The structural similarity of the parent compounds creates favorable conditions for the formation of solid solutions in the investigated system.

2. Experimental

2.1. Materials and Synthesis

For the investigation of physicochemical interactions in the system, the initial compounds Ag_8SnSe_6 and Ag_7SnSe_5I were preliminarily synthesized (10 g each). The syntheses were carried out by direct melting of stoichiometric mixtures of high-purity elemental substances (Ag rod, 99.997%; Sn ingot, 99.999%; Se granules, 99.999%; I powder, 99.999%) in evacuated sealed quartz ampoules under vacuum conditions (10^{-2} Pa).

Taking into account the high volatility of elemental iodine, the synthesis of Ag_7SnSe_5I was performed as follows: the required amounts of silver, tin, and selenium were first loaded into the ampoule and weighed, after which iodine was introduced while the ampoule was cooled in ice water. The ampoule was then evacuated and sealed.

Since the saturated vapor pressures of iodine (T_{boil} = 457 K) and selenium (T_{boil} = 958 K [40]) are high at melting temperatures, the syntheses were performed in an inclined furnace. Quartz ampoules of approximately 15 cm in length and 1.2–1.3 cm in inner diameter were used. During synthesis, a portion of the ampoule (~6 cm) was kept outside the furnace, forming a “cold” zone. In order to regulate the vapor pressure of volatile components and prevent ampoule rupture, this part was additionally cooled with water. The lower part of the furnace (“hot” zone) was gradually heated to a temperature 30–50 °C above the melting point of the synthesized compound.

During heating, the volatile components of both systems migrated to the upper “cold” part of the ampoule, where they condensed and subsequently returned to the reaction zone. As the reaction proceeded, the amount of volatile components gradually decreased and was almost completely exhausted within 1–2 h, which was visually observed. Thereafter, the ampoules were completely placed inside the furnace, annealed for approximately 1 h, and subsequently cooled together with the switched-off furnace.

The phase purity of the synthesized samples was examined by differential thermal analysis (DTA), X-ray diffraction analysis (XRD), and scanning electron microscopy (SEM).

Analysis of the DTA curve of synthesized Ag_8SnSe_6 (Fig. 1) demonstrated that the compound undergoes a polymorphic transformation at 355 K and melts at 1015 K, which is in good agreement with the literature data reported above [23].

In contrast, the heating curve of Ag_7SnSe_5I exhibited a single pronounced thermal effect at 995 K, which was attributed to its congruent melting temperature (Fig. 1).

X-ray diffraction analysis also confirmed the single-phase nature of the synthesized compounds. For Ag_8SnSe_6, the obtained parameters (space group $Pmn2_1$, a = 0.79170(6), b = 0.78217(7), c = 1.10455(7) nm) were in good agreement with the literature data [30]. For Ag_7SnSe_5I, the parameters of the cubic crystal structure (space group $F\bar{4}3m$, a = 1.1164 nm) were refined from the powder diffraction pattern using the Le Bail method. These data are consistent with the lattice parameters reported for Ag_7GeSe_5I (a = 1.10019 nm). The increase in the lattice parameter from 1.10019 nm for Ag_7GeSe_5I to 1.1164 nm for Ag_7SnSe_5I is associated with the substitution of germanium atoms by larger tin atoms.

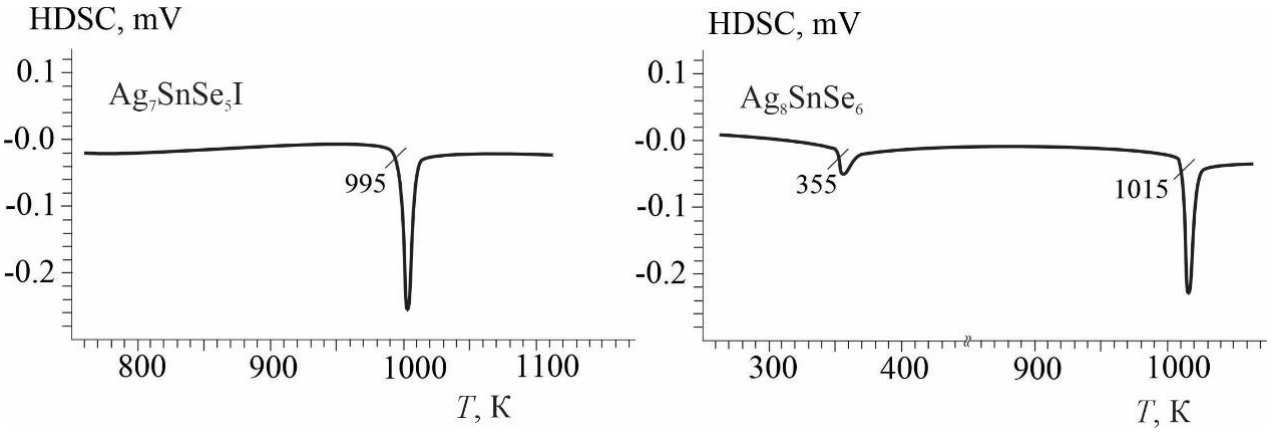

Fig. 1. DTA heating curve for the compounds of Ag_7SnSe_5I and Ag_8SnSe_6

Alloys of the Ag_8SnSe_6–Ag_7SnSe_5I system were prepared by melting the identified parent compounds in various ratios in sealed quartz ampoules. Two series of samples were synthesized for each composition. Samples of series I were annealed at temperatures 30–50 °C below the solidus temperature for 500 h, followed by cooling together with the switched-off furnace. Samples of series II were quenched from 900 K by rapid cooling in ice water.

2.2. Methods

The investigations were carried out using differential thermal analysis (DTA), X-ray diffraction analysis (XRD), scanning electron microscopy (SEM), and microhardness measurements.

DTA measurements were performed in evacuated quartz ampoules within the temperature range from room temperature to 1400 K at a heating rate of 10 $K \cdot min^{-1}$ using a NETZSCH 404 F1 Pegasus System differential scanning calorimeter equipped with platinum–rhodium thermocouples. Experimental data were processed using NETZSCH Proteus software. The temperature determination error was approximately ±2 K.

X-ray diffraction analysis was carried out at room temperature using a BRUKER D8 ADVANCE diffractometer with $CuK\alpha_1$ radiation. Indexing of powder diffraction

patterns was performed using Topas V3.0 software (Bruker). The errors of the lattice parameters were determined using the software package of the diffractometer and are given in parentheses.

Microhardness measurements of slowly cooled and quenched alloys were performed using a PMT-3 microhardness tester equipped with a Vickers indenter (a regular four-sided pyramid with an apex angle of 136°) under a load of 50 g. The measurements were carried out at room temperature. Ten measurements were performed for each sample, and the average value of the indentation diagonal was calculated. The numerical values of microhardness were determined according to the following formula.

3. Results and discussion

Figure 2 shows the powder diffraction patterns of several slowly cooled alloys (series I) of the investigated system. As can be seen, the XRD data confirm the formation of wide solid-solution regions. The diffraction patterns of alloys containing >40 mol% Ag_7SnSe_5I are fully indexed within the cubic lattice of the Ag_7SnSe_5I compound. In contrast, alloys containing ≤25 mol% Ag_7SnSe_5I exhibit diffraction patterns identical to those of RT-Ag_8SnSe_6, indicating that these compositions belong to the homogeneity region of the γ-phase. Alloys containing 25–40 mol% Ag_7SnSe_5I display reflections corresponding to both parent compounds and are therefore two-phase.

The alloys of series II exhibited diffraction patterns characteristic of the cubic structure of Ag_7SnSe_5I. As an example, the powder diffraction pattern of the alloy containing 30 mol% Ag_7SnSe_5I is presented in Fig. 3.

The concentration dependences of microhardness are presented in Fig. 4. As can be seen, the microhardness of the quenched samples (series II, δ-phase with cubic structure) exhibits a smooth increasing trend relative to the parent compounds, which is characteristic of systems forming continuous substitutional solid solutions.

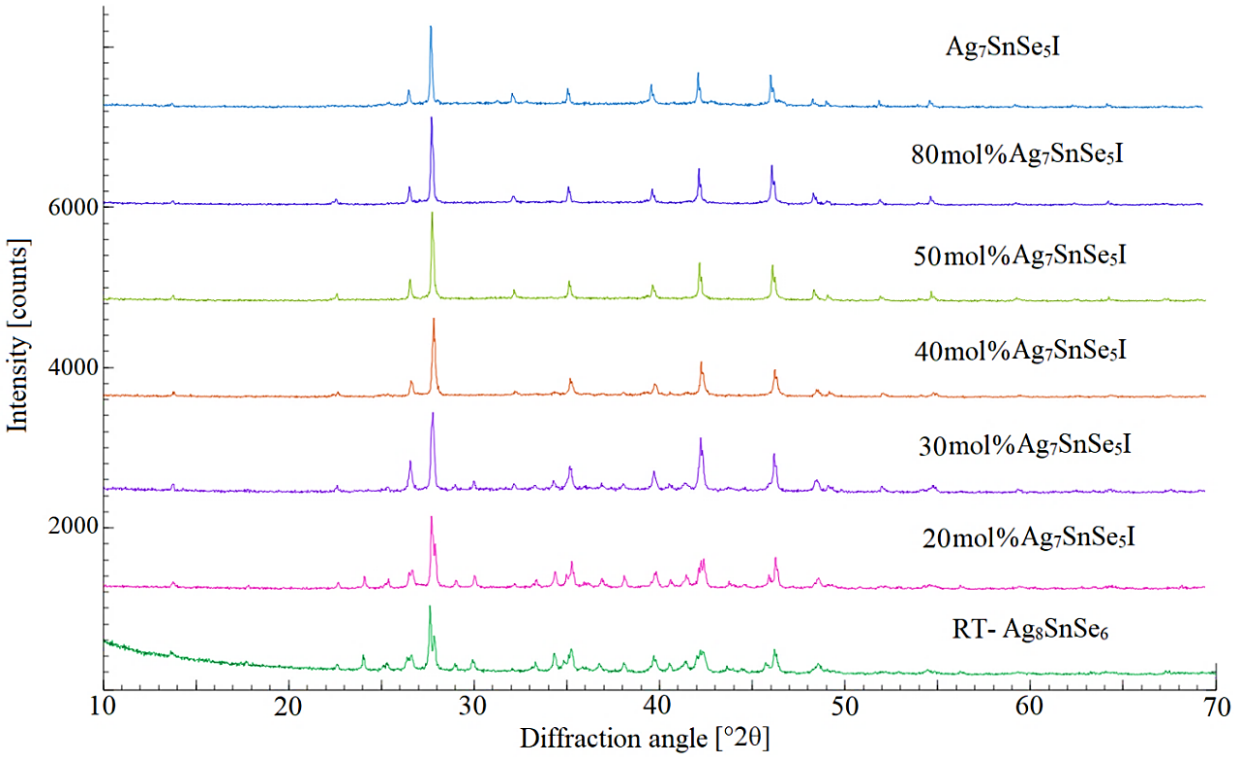

Fig 2. Powder X-ray diffraction patterns of slowly cooled alloys of the Ag_8SnSe_6–Ag_7SnSe_5I system

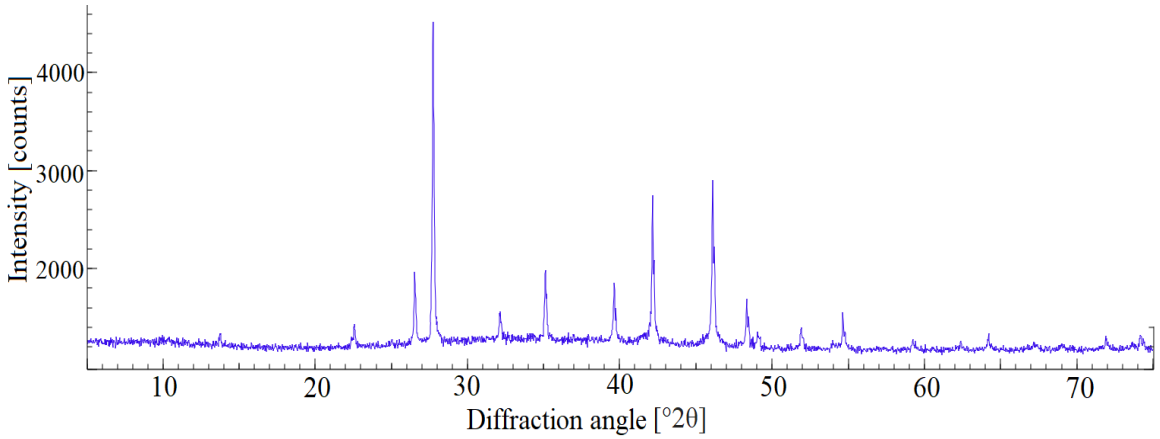

Fig 3. Powder X-ray diffraction pattern of the alloy containing **30 мол % Ag_7SnSe_5I** quenched from 800 K into cold water.

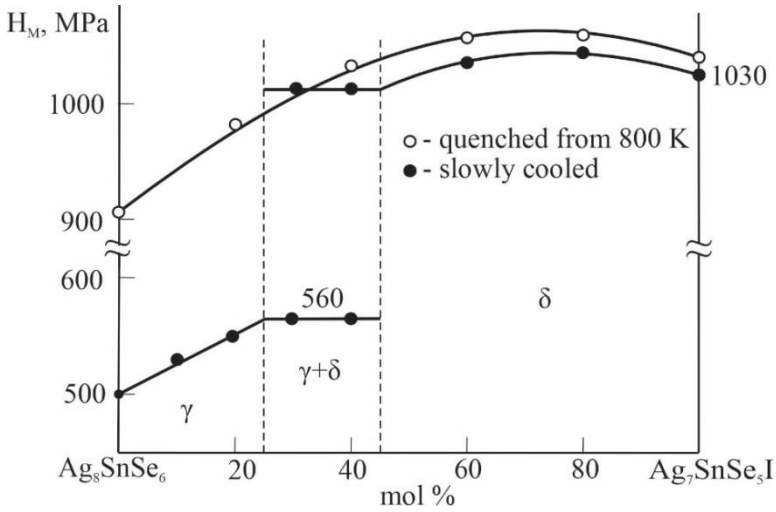

Fig. 4. Composition dependence of the microhardness of alloys in the Ag_8SnSe_6–Ag_7SnSe_5I system

Table 1.. DTA data and microhardness measurements for alloys of the Ag_8SnSe_6-Ag_7SnSe_5I system

Composition, mol % Ag_7SnSe_5I	Microhardness		Thermal effects, K
	Slowly annealed samples	Samples quenched from 900 K.	
0	500	910	355; 1015
10	535	-	342; 1012
20	550	980	331-340; 1009-1014
30	560; 1010	-	331; 1007-1013
40	560; 1010	1035	1005-1012
60	1035	1060	1001-1007
80	1050	1065	998-1005
90	-	-	996
100	1030	1040	995

The concentration dependence of microhardness for the slowly cooled alloys (series I) demonstrates a somewhat different behavior. The microhardness of RT-Ag_8SnSe_6 (black circles in Fig. 4) increases within the composition range of 0–25 mol% Ag_7SnSe_5I and remains nearly constant within the two-phase γ + δ region. In this composition range, the microhardness of the δ-phase also remains constant. This confirms the invariability of the compositions of both phases within the indicated two-phase region.

The microhardness behavior in the Ag_7SnSe_5I-rich region is similar to that observed for the quenched samples, confirming the single-phase nature of the δ-phase at compositions containing more than 45 mol% Ag_7SnSe_5I.

Based on the DTA data, together with the results of microhardness measurements (Table 1), as well as XRD and SEM analyses, the T–x phase diagram of the Ag_8SnSe_6–Ag_7SnSe_5I system was constructed (Fig. 5).

The phase regions presented in Fig. 5 are also confirmed by SEM analysis. As an example, SEM micrographs of alloys #1, #2, and #3 are shown in Fig. 6. As can be seen, the SEM image of alloy #2 reveals the presence of two phases (γ and δ), whereas alloys #1 and #3 are single-phase.

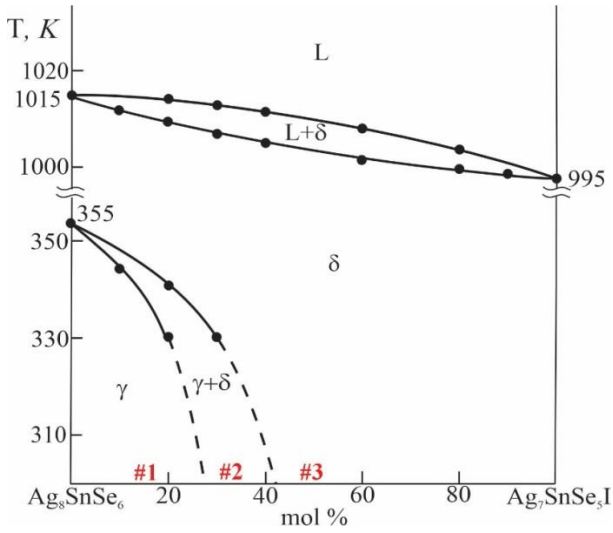

Fig. 5. Ag_8SnSe_6-Ag_7SnSe_5I phase diagram

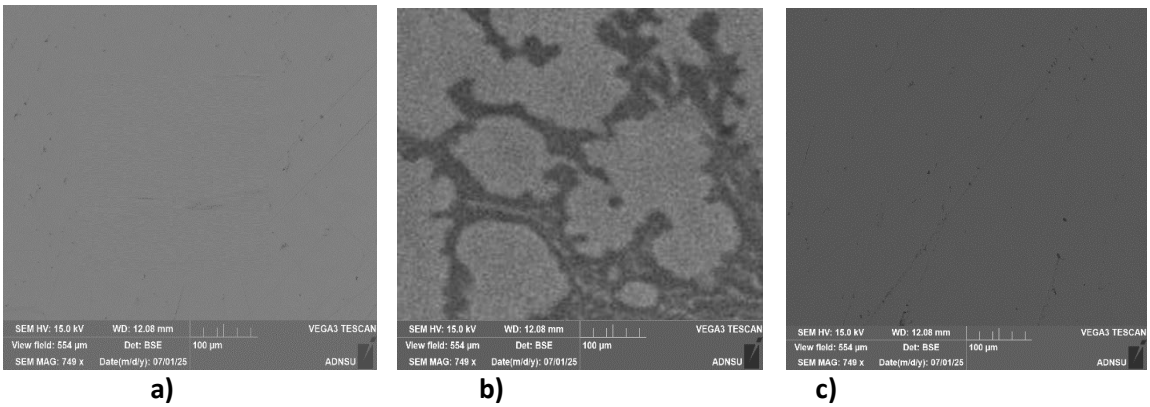

Fig. 6. SEM micrographs of alloys #1 (a), #2 (b), and #3 (c) of the Ag_8SnSe_6-Ag_7SnSe_5I system

Conclusion

Thus, new data on phase relations in the Ag_8SnSe_6-Ag_7SnSe_5I system have been obtained using differential thermal analysis, X-ray diffraction, and microhardness measurements. The Ag_8SnSe_6-Ag_7SnSe_5I system was found to exhibit a continuous series of solid solutions with cubic structure between Ag_7SnSe_5I and HT-Ag_8SnSe_6 as well as limited solid solutions based on RT-Ag_8SnSe_6. It was shown that solid-solution formation is accompanied by a decrease in the polymorphic transition temperature of Ag_8SnSe_6, leading to stabilization of the high-temperature ion-conducting phase at and below room temperature. The obtained solid solutions are of interest as potential environmentally friendly thermoelectric materials with anomalously low thermal conductivity and as mixed ionic–electronic conductors.

Reference

1. Hahn H., Schulze H., Sechser L. Über einige ternäre Chalkogenide vom Argyrodit-Typ. *Naturwissenschaften*. 1965. V. 52. № 11. P 451, in German. https://doi.org/10.1007/BF00627053
2. Gorochov O. Les composés Ag_8MX_6 (M = Si, Ge, Sn et X = S, Se, Te). *Bull. Soc. chim. Fr.* 1968. V. 101. № 6. P. 2263-2275, in French.
3. Laqibi M., Cros B., Peytavin S., M. Ribes, New silver superionic conductors Ag_7XY_5Z (X = Si, Ge, Sn; Y = S, Se; Z = Cl, Br, I) – Synthesis and electrical studies. *Solid State Ion.* 1987. V. 23. № 1-2. P. 21-26. https://doi.org/10.1016/0167-2738(87)90077-4
4. Babanly M.B., Yusibov Y.A., Imamaliyeva S.Z. et al. Phase diagrams in the development of the argyrodite family compounds and solid solutions based on them. *J. Phase Equilib. diffus.* 2024. V. 45. P. 228-255. doi:10.1007/s11669-024-01088-w.
5. Lin S., Li W., Pei Y. Thermally insulative thermoelectric argyrodites. *Mater. Today*. 2021. V. 48. P. 198-213 doi: 10.1016/j.mattod.2021.01.007
6. Zhang X., Zhang C.L., S. Lin et al. Thermoelectric properties of n-type Nb-doped Ag_8SnSe_6. *J. Appl. Phys.* 2016. V. 119. № 13. P. 135101. https://doi.org/10.1063/1.4945033
7. Yang C., Xia Y., XuL. et al. Enhancement of thermoelectric performance of argyrodite Ag_8GeSe_6 via isoelectronic substitution of Sn for Ge. *Chem. Eng. J.* 2021. V. 426. P. 131752. doi:10.1016/j.cej.2021.131752
8. Ghata A., Eckert P.L., Böger T. et al. Influence of Cu^+ Substitution on the Structural, Ionic, and Thermal Transport Properties of $Ag_{8-x}Cu_xGeS_6$ Argyrodites. *Chem. Mater*. 2025. V. 37. № 17. P. 6900–6911. DOI: 10.1021/acs.chemmater.5c01679
9. Zaman T., Ullah M., Chaudhry A.R., et al. Optoelectronic, thermoelectric, and elastic properties of Cu_6PSe_5X (X = Br, I) argyrodites using density functional theory. *Phys. Scr.* 2024. V. 99. № 11. P. 1159106. DOI: 10.1088/1402-4896/ad886f
10. Bilanych V.S., Babilya M.I., Korovska D.M. et al. Mechanical properties of superionic ceramics based on $(Cu_{1-x}Ag_x)_7GeSe_5I$ solid solutions. *Semicond. Phys. Quantum Electron. Optoelectron.* 2021. V. 24. № 4. P. 372-377. doi:10.15407/spqeo24.04.372
11. Pogodin A.I., Filep M., Malakhovska T. et al. Recrystallization effect on mechanical parameters and increase in Ag^+ ionic conductivity in $Ag_7(Si_{1-x}Ge_x)S_5I$ ceramic materials. *Solid State Sci.* 2023. V. 140. P. 107203. DOI: 10.1016/j.solidstatesciences.2023.107203
12. Sardarly R.M., Ashirov G.M., Mashadiyeva L.F. et al. Ionic conductivity of the Ag_8GeSe_6 compound. *Mod. Phys. Lett.* B. 2022. V. 36. № 32. P. 2250171 https://doi.org/10.1142/S0217984922501718
13. Sardarly R.M., Babanly M.B., Aliyeva N.T. et al. Obtaining and Measuring Impedance Characteristics of the Ag_8SiSe_6 Compound. *East Eur. J. Phys.* 2025. № 1. P. 233-239. https://doi.org/10.26565/2312-4334-2025-1-24
14. Munsif M., Neffati R., Shah M. et al. First principles study of the structural, mechanical, and optical properties of argyrodite-structured Ag_6PS_5X (X = Br, I) compounds. *Solid State Commun.* 2023. V. 371. P. 115245
15. Pogodin A., Filep M., Shender I. et al. $Ag_{7.23}SnS_{5.44}I_{0.50}$ - a new argyrodite-like conductor with promising optical and electrical performance. *Acta Mater.* 2026. V. 304. P. 121803.
16. Yeh L.-Y., Cheng K-W. Modification of Ag_8SnS_6 Photoanodes with Incorporation of Zn Ions for Photo-Driven Hydrogen Production. *Catalysts.* 2021. V. 11. № 3. P. 363. https://doi.org/10.3390/catal11030363
17. Yang M., Shao G., Wu B. et al. Irregularly Shaped Bimetallic Chalcogenide Ag_8SnS_6 Nanoparticles as Electrocatalysts for Hydrogen Evolution. *ACS Appl. Nano Mater.* 2021. V. 4. № 7. P. 6745-6751. https://doi.org/10.1021/acsanm.1c00769
18. Zhu L.Z., Xu Y.F., Zheng H.Y. et al. Application of Facile Solution-Processed Ternary Sulfide Ag_8SnS_6 as Light Absorber in Thin Film Solar Cells. *Sci.*

China Mater. 2018. V. 61. P. 1549-1556. https://doi.org/10.1007/s40843-018-9272-3
19. Cantor B. Exploring Multicomponent Phase Space to Discover New Materials. *J. phase equilib. diffus*. 2024. V. 45. P. 188–218. doi:10.1007/s11669-024-01131-w
20. Zipoli F., Viterbo V., Schilter O. et al. Prediction of Phase Diagrams and Associated Phase Structural Properties. *Ind. Eng. Chem. Res.* 2022. V. 61. № 24. P. 8378–8389. https://pubs.acs.org/doi/10.1021/acs.iecr.2c00355
21. Saka H. *Introduction to phase diagrams in materials science and engineering*. World Scientific Publishing Co. 2020. 188 p
22. Babanly M.B., Mashadieva L.F., Imamaliyeva S.Z. et al. Complex copper-based chalcogenides: a review of phase equilibria and thermodynamic properties. *Condens. Matter Interphases*. 2024. V. 26. № 4. P. 579-619. doi: 10.17308/kcmf. 2024.26/12367.
23. Babanly M.B., Mashadiyeva L.F., Imamaliyeva S.Z. et al. Thermodynamic properties of complex copper chalcogenides. *Chem. Prob.* 2024. № 3. P. 243-280. doi: 10.32737/2221-8688-2024-3-243-280
24. Aslanli S.R., Alverdiyev I.J., Imamaliyeva S.Z. et al. Phase Relations in the Ag_2S-Ag_8SiS_6-Ag_8SnS_6 System and Thermodynamic Properties of Polymorphic Transitions of Argyrodite Phases. *International J. Thermophysics*. 2025. V. 46. P 26-41 https://doi.org/10.1007/s10765-025-03501-z
25. Aslanli S.R., Babanly K.N., Imamaliyeva S.Z. et al. System Ag_2Se-Ag_8SiSe_6-Ag_8SnSe_6. *Russ. Chem. Bull.* 2025. V. 74. № 5. P. 1237–1246. doi:10.1007/s11172-025-4618-2.
26. Amiraslanova A.J., Mammadova A.T., Imamaliyeva S.Z. et al. The $6Ag_2Se+Ag_8GeTe_6 \leftrightarrow 6Ag_2Te+Ag_8GeSe_6$ reciprocal system. *Russ. J. Inorg. Chem.* 2023. V. 68. № 8. P. 1054-1064. DOI: 10.1134/S0036023623601046
27. Poladova A.N., Huseynova I.F., Alverdiyev I.J. et al. Phase equilibria and high-entropy alloys in the Cu_8GeSe_6-Ag_8GeS_6 system. *Russ. J. Inorg. Chem.* 2025. V. 70. № 11. P. 1778-1784
28. Bayramova U.R., Poladova A.N., Mashadiyeva L.F. Synthesis and x-ray study of the $Cu_8Ge_{(1-x)}Si_xS_6$ solid solutions. *New Mater. Compd. Appl*. 2022. V. 6. № 3. P. 276-281
29. Amiraslanova A.J., Babanly K.N., Imamaliyeva S.Z. et al. Phase equilibria in the Ag_8SiSe_6- Ag_8SiTe_6 system and characterization of solid solutions $Ag_8SiSe_{6-x}Te_x$. *Appl. Chem. Eng.* 2023. V. 6. № 2. P. 1-9. doi: 10.24294/ace.v6i2.2162
30. Alverdiyev I.J., Imamaliyeva S.Z., Akhmedov E.I. et al. Thermodynamic properties of some ternary compounds of the argyrodite family. *Azerb. Chem. J.* 2023. № 4. P. 21–30. doi: 10.32737/0005-2531-2023-4-21-30.
31. Amiraslanova A.J., Babanly K.N., Imamaliyeva S.Z. et al. Phase relations in the Ag_8SiS_6-Ag_8SiTe_6 system and characterization of solid solutions. *Azerb. Chem. J.* 2023. № 2. P. 169-177
32. Amiraslanova A.J., Babanly K.N., Imamaliyeva S.Z. et al. Phase relations in the $6Ag_2Se+Ag_8SiTe_6$ $6Ag_2Te+Ag_8SiSe_6$ reciprocal system. *Azerb. Chem. J.* 2023. № 3. P. 6-17
33. Bayramova N.A., Huseynova I.F., Melikova E.T., Imamaliyeva S.Z. Phase relations in the AgI-Ag_7GeSe_5I-$GeSe_2$ system. *Baku State Univ. J. Chem. Mater. Sci.* 2025. V. 2. № 3. P. 36-42. DOI: 10.30546/209501.201.2025.2.003.012
34. Huseynova I.F., Bayramova N.A., Imamaliyeva S.Z. et al. Phase equilibria in the Ag_8GeSe_6-Ag_7GeSe_5I-$GeSe_2$ system. *Russ. J. Inorg. Chem.* 2025. V. 70. № 11. P. 1793–1802. doi: 10.1134/S0036023625602533
35. Bayramova N.A., Huseynova I.F., Balakishiyeva G.B. et al. Thermodynamic investigation of the Ag_7GeSe_5I compound and $Ag_{8-x}GeSe_{6-x}I_x$ solid solutions by the EMF method with solid electrolyte. *Chem. Prob.* 2026. № 4. P. 540-552. DOI: 10.65382/2221-8688-2026-4-540-552
36. Huseynova I.F., Bayramova N.A., Imamaliyeva S.Z. et al. Phase Relations and Crystallization Processes in the Ag_2Se-AgI-$GeSe_2$ System. *J. Phase Equilib. Diffus.* 2026. https://doi.org/10.1007/s11669-026-01258-y
37. Fichet R.O., J. Rivet J. Flahaut J. Description du système ternaire Ag–Sn–Se. *Less-Common Met.* 1988. V. 138. P. 241-261. https://doi.org/10.1016/0022-5088(88)90113-0
38. Yusibov Yu.A., Alverdiev I.Dzh., Mashadieva L.F. et al. Experimental Study and 3D Modeling of the Phase Diagram of the Ag–Sn–Se System. *Russ. J. Inorg. Chem.* 2018. V. 63. № 12. P. 1622–1635. https://doi.org/10.1134/S0036023618120227
39. Gulay L.D., Olekseyuk I.D., Parasyuk O.V. Crystal structure of β-Ag_8SnSe_6. *J. Alloys Compd.* 2002. V. 339. P. 113-117.
40. Emsley J. *The Elements*. second edition. London: Clarendon Press. 1993. 256 P.

$Ag_{8-x}SnSe_{6-x}Ix$ BƏRK MƏHLULLARININ SİNTEZİ VƏ FİZİKİ-KIMYƏVİ TƏDQİQİ

N.A. Bayramova, İ.F. Hüseynova, K.N.Babanlı, N.M.Allazova, N.B.Babanlı, M.Bulanova, S.Z.İmaməliyeva

Ag_8SnSe_6-Ag_7SnSe_5I sistemində faza tarazlıqlarının diferensial termiki və rentgenfaza analizlərilə tədqiqinin nəticələri təqdim olunmuşdur. Müəyyən edilmişdir ki, Ag_8SnSe_6–Ag_7SnSe_5I sistemi Ag_7SnSe_5I ilə Ag_8SnSe_6 birləşmələrinin yüksək temperaturlu kubik modifikasiyası arasında arasıkəsilməz bərk məhlul məhlulların, eləcə də sonuncu birləşmənin aşağı temperaturlu modifikasiyasının əsasında məhdud bərk məhlulların əmələ gəlməsi ilə xarakterizə olunur. Bərk məhlulların əmələ gəlməsi Ag_8SnSe_6 birləşməsinin polimorf keçid temperaturunun azalmasına və otaq temperaturunda yüksək temperaturlu kubik fazasının stabilləşməsinə gətirib çıxarır. Əldə edilən nəticələr Ag_8SnSe_6–Ag_7SnSe_5I sistemində Se↔I əvəzlənməsi ilə bərk məhlulların kristal yetişdirilməsi baxımından maraq doğurur.

Açar sözlər: argirodit ailəsi birləşmələri, gümüş-qalay selenoyodidi, faza tarazlıqları, bərk məhlullar, T–x diaqramı.